20 Years Unleashing the Power of HPC

SC2008

2008 Chair
Patricia Teller
Austin, Texas

2008

Notable Systems First mentioned this year in the proceedings:

- Road Runner - IBM Cell BE Blades
- Jaguar - Cray XT4
- Ranger - Sun Constellation Cluster
- NCSA Tungsten Dell and Mercury IBM/Intel

Notable Processors:

- IBM PowerXCell 8i
- Tilera 64-core mesh-commected chip
- Intel 80-core Terascale processor
- Sun UltraSparc T2+ Victoria Falls

Noteworthy Architecture Topics:

- Hybrid-processor systems
- GPU performance and algorithms
- Optimizing for Power Performance
- Live Process Migration

Notable Operating Systems:

- Catamount

Notable Languages:

- CUDA

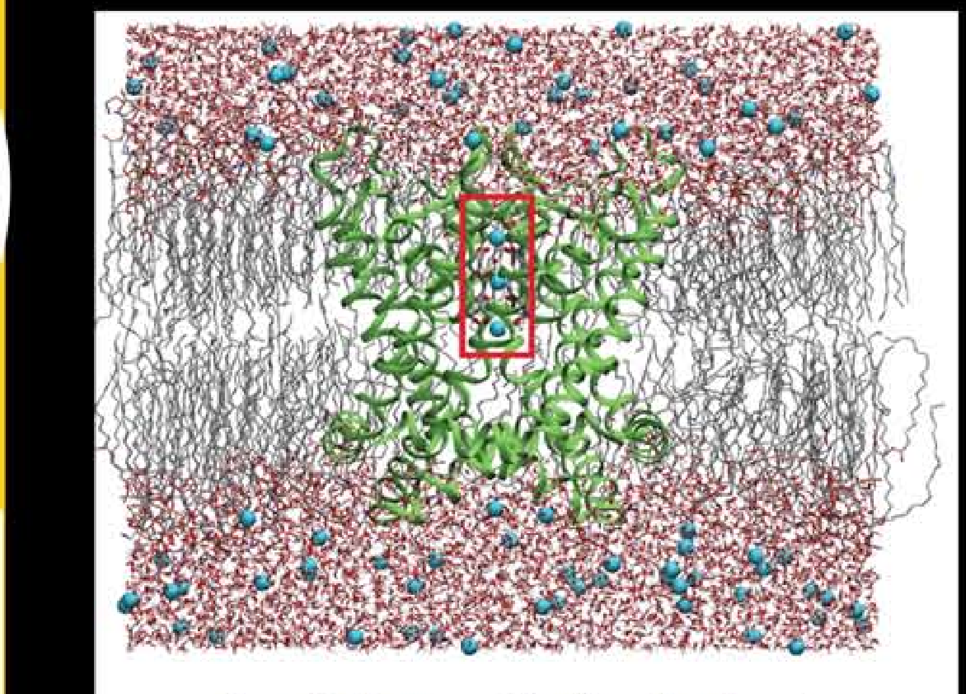

Figure 2. Ion permeation through a channel.

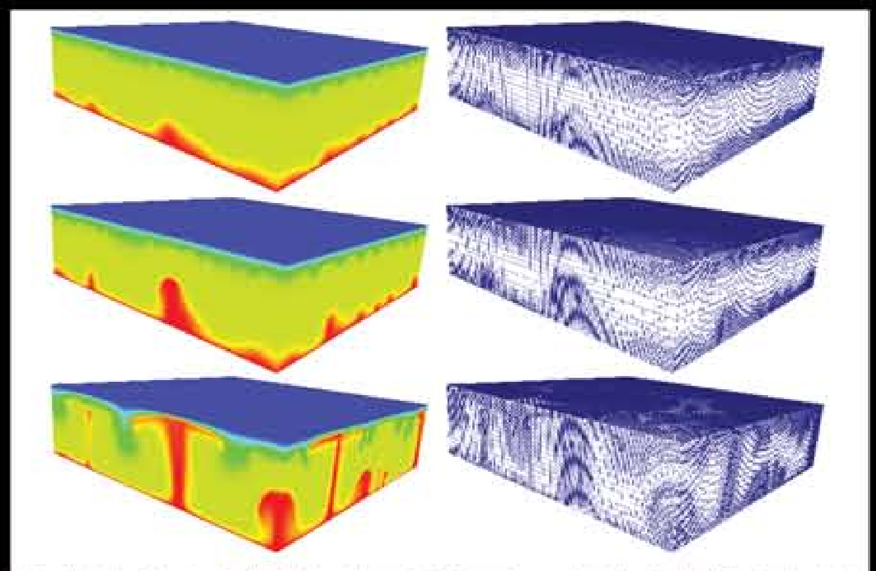

Fig. 1. Illustration of dynamic mesh adaptation for mantle convection. The figure shows snapshots of the thermal field T at three time instants (left column) and corresponding adapted meshes (right column). The mesh resolves the rising plumes as well as the instabilities at the top layer. The elements span levels 4 to 9 in octree depth.

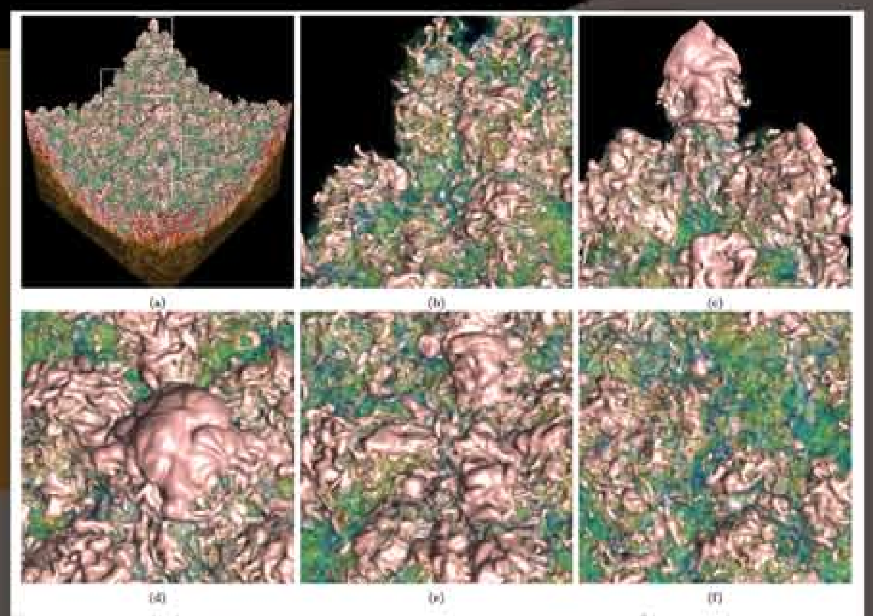

Figure 10: Rendering of a RMI data set. (a): an overview of the data. (b) - (f): five 512^2 zoom-in views cropped from a 4096^2 image output. The high-resolution, high-precision composited images allow clear observation of fine details in the large volume data set.

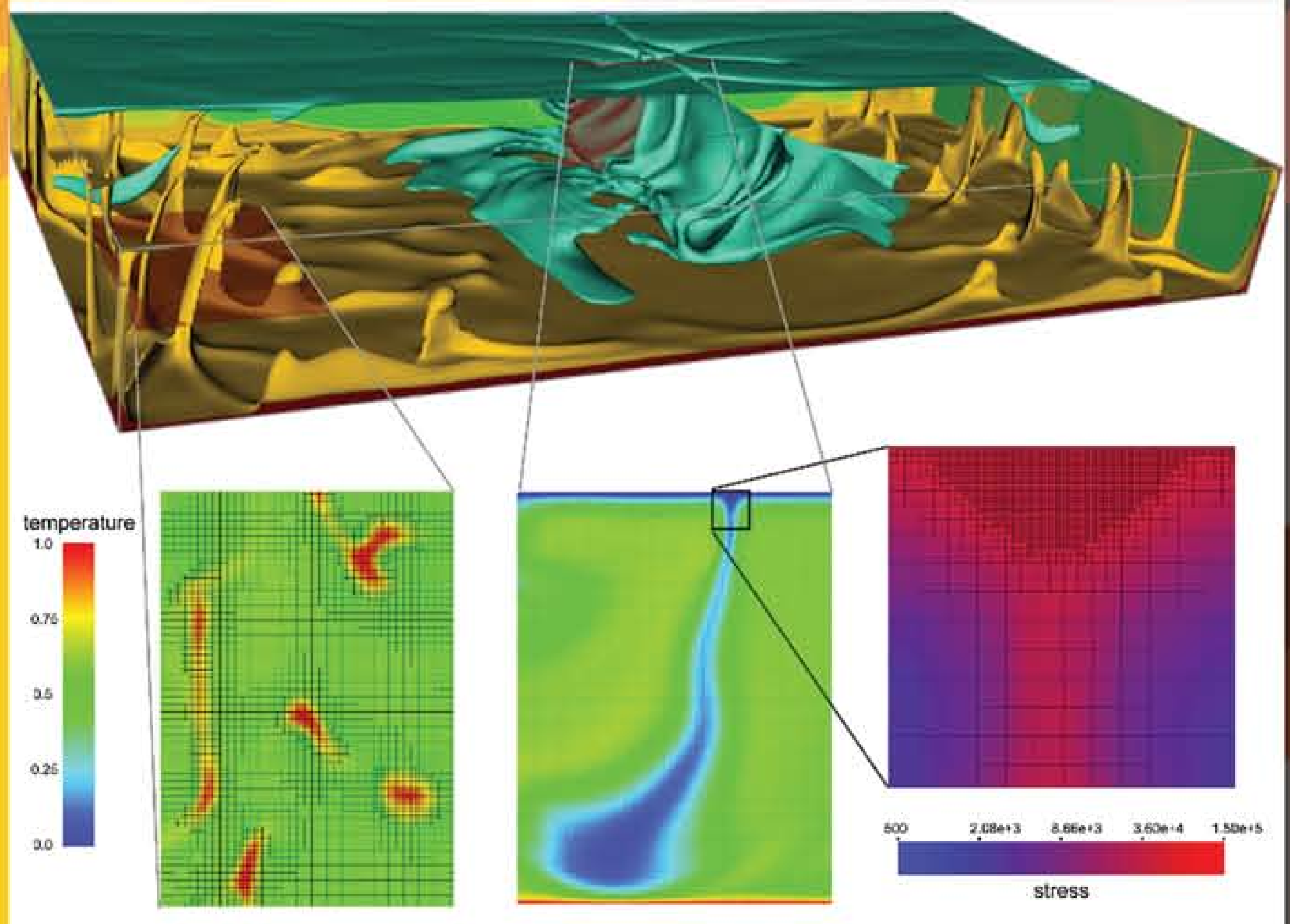

Fig. 11. Mantle convection with yielding. Top: Temperature isosurfaces at $T = 0.3$ (cyan), $T = 0.8$ (orange). Bottom left: Horizontal slice of temperature showing that grid refinement follows the temperature gradient. Bottom center: Vertical slice of temperature showing the downwelling slab and the yielding zone. Bottom right: A zoom-in of the yielding zone, where the finest grid of ~ 1.5 km resolution covers the region of highest stress.

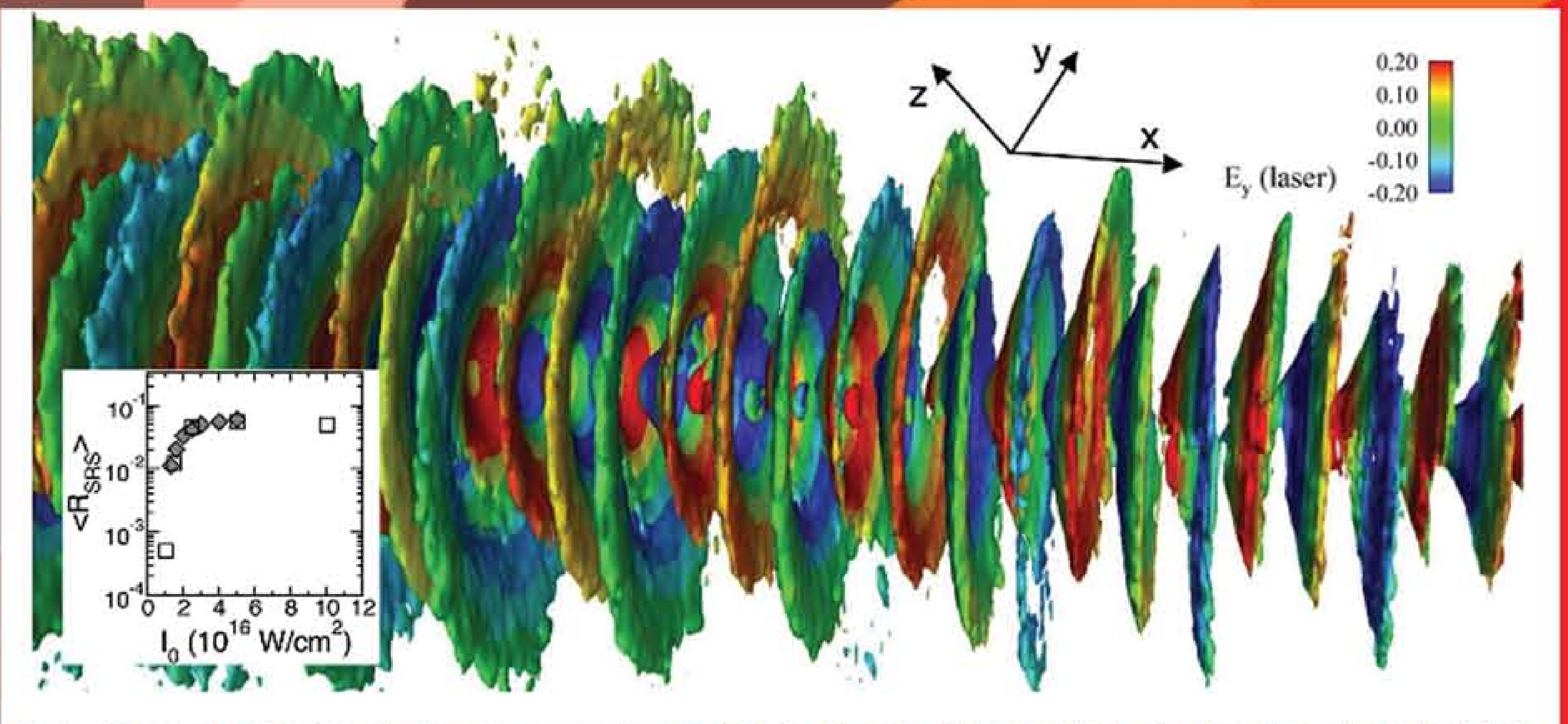

Fig. 1. Bowing and self-focusing of electron plasma waves from a 3d SRS simulation of a $f/4$ speckle. Displayed are isosurfaces of longitudinal electric field E_x (indicating the presence of electron plasma waves) with color indicating laser field (E_y). In the nonlinear evolution of SRS, the source for SRS backscatter (proportional to E_xE_y) loses coherence, as represented by the multi-colored isosurfaces. Inset: SRS reflectivity as a function of incident laser peak intensity [1] for laser and plasma conditions comparable to Problems 1 and 2. Squares represent reflectivity obtained from runs on a homogeneous cluster of Opteron cores; diamonds are from a *suite of calculations run on Roadrunner with higher phase-space fidelity*. Both sets of simulations used 136×10^6 voxels. As expected, the observed saturated reflectivity (the plateau) is the same, but the lower noise afforded by higher fidelity on Roadrunner leads to reflectivity onset at a slightly lower intensity, as predicted by theory [2]. These science runs are a stringent test of correctness of the Cell implementation of VPIC. Moreover, they allow better characterization of the nonlinear onset and saturation of SRS in NIF-like plasma conditions, the key physics to be implemented in reduced physics models like pF3D.